Gold Nanoclusters

Deutsche Ausgabe: DOI: 10.1002/ange.201503893
Internationale Ausgabe: DOI: 10.1002/anie.201503893

A Near-Infrared-Emissive Alkynyl-Protected Au_{24} Nanocluster**

Xian-Kai Wan, Wen Wu Xu, Shang-Fu Yuan, Yi Gao, Xiao-Cheng Zeng, and Quan-Ming Wang**

Abstract: *An alkynyl-protected gold nanocluster $[Au_{24}(C{\equiv}C\text{-}Ph)_{14}(PPh_3)_4](SbF_6)_2$ has been prepared by a direct reduction method. Single-crystal X-ray diffraction reveals that the molecular structure contains a Au_{22} core that is made of two Au_{13}-centered cuboctahedra that share a square face. Two staple-like PhC≡C−Au−C≡CPh motifs are located around the center of the rod-like Au_{22} core. This Au_{24} nanocluster is highly emissive in the near-infrared region with $\lambda_{max} = 925$ nm and the nature of the HOMO–LUMO transition is investigated by time-dependent DFT calculations.*

Gold nanoclusters attract increasing attention because of their importance in fundamental research and their potential applications.[1–5] In contrast to thiolate-[6–16] or phosphine-protected gold nanoclusters,[17–21] few examples of alkynyl-protected have been reported.[22–25] An alkynyl ligand contains a C≡C group that, upon coordination to metal centers, can function as both a σ and π donor. This dual functionality could give rise to interesting features in the resulting products. First, a new gold nanocluster core may be formed as a result of ligand control. Second, the interfacial structure between the gold core and the alkynyl ligand may be different from that of thiolate-protected gold nanoclusters. Finally, the unsaturated nature of the triple bond in alkynyl ligands can bring new properties to the clusters. The synthesis of alkynyl-protected gold nanoclusters has been achieved only recently. Tsukuda et al. found that Brust method[26] was not applicable in the preparation of alkynyl-protected gold nanoclusters so they synthesized $Au_n(PhC{\equiv}C)_m$ by direct ligation of phenylacetylene to preformed Au clusters (Au:PVP; PVP = poly(vinylpyrrolidone)).[22] Konishi et al. prepared a mixed-ligand-protected $[Au_8(dppp)_4(C{\equiv}CR)_2]^{2+}$ (dppp = 1,3-bis(diphenylphosphanyl)propane) through the dialkynylation of preformed $[Au_8(dppp)_4]^{2+}$.[23] More recently, we have shown that the direct reduction of gold alkynyl precursors with sodium borohydride led to the isolation of $[Au_{19}(C{\equiv}CPh)_9(Hdppa)_3](SbF_6)_2$ (Hdppa = *N*,*N*-bis-(diphenylphosphino)-amine) and $[Au_{23}(C{\equiv}CPh)_9(PPh_3)_6](SbF_6)_2$.[24,25] Similar to the gold–thiolate staple motif,[11] V-shaped PhC≡C−Au−C_2(Ph)−Au−C≡CPh motifs were found in both Au_{19} and Au_{23} clusters.[24,25] With these results in mind we set out to investigate if other types of gold–alkynyl staple moieties exist in gold nanoclusters.

Herein, we report the synthesis and structure determination of $[Au_{24}(C{\equiv}CPh)_{14}(PPh_3)_4](SbF_6)_2$ (**1**). The species has a unique Au_{22} core structure composed of two centered cuboctahedral Au_{13} units which share a square face. Two extending Au atoms are attached to the core through new gold–alkynyl binding motifs PhC≡C−Au−C≡CPh. Interestingly, this Au_{24} cluster is highly emissive in the near-infrared region in solution at room temperature.

Cluster **1** was prepared from the reduction of PhC≡CAu and $Ph_3PAuSbF_6$ by $NaBH_4$ in $CHCl_3$. The composition of **1** was determined by Fourier transform ion-cyclotron-resonance MS (FT-ICR-MS; Figure 1), which showed a single signal at *m*/*z* 3595.56 corresponding to the molecular ion $[Au_{24}(C{\equiv}CPh)_{14}(PPh_3)_4]^{2+}$. The detected isotopic pattern of $[Au_{24}(C{\equiv}CPh)_{14}(PPh_3)_4]^{2+}$ is in good agreement with the simulated pattern (Figure 1, inset).

The structure of **1** was determined by single-crystal X-ray diffraction.[27] The centrosymmetric structure contains a Au_{22} core and two PhC≡C−Au−C≡CPh motifs and the core is further protected by 14 C≡CPh and 4 PPh_3 ligands (Figure 2a). Four surface gold atoms are each terminally coordinated by a PPh_3 ligand. The PPh_3 ligands are in very similar environments, as confirmed by the ^{31}P NMR spectrum

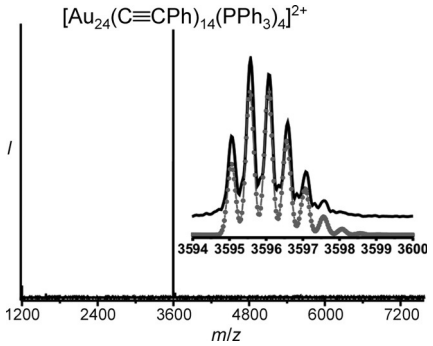

Figure 1. Mass spectrum of the Au_{24} cluster. Inset: Enlarged portion of the spectrum showing the measured (black, solid trace) and simulated (gray, dotted trace) isotopic distribution patterns of the species $[Au_{24}(C{\equiv}CPh)_{14}(PPh_3)_4]^{2+}$.

[*] X.-K. Wan, S.-F. Yuan, Prof. Dr. Q.-M. Wang
State Key Lab of Physical Chemistry of Solid Surfaces
Department of Chemistry, College of Chemistry and Chemical Engineering, Xiamen University
Xiamen, 361005 (P.R. China)
E-mail: qmwang@xmu.edu.cn
Dr. W. W. Xu, Prof. Y. Gao
Shanghai Institute of Applied Physics
Chinese Academy of Sciences, Shanghai, 201800 (China)
E-mail: gaoyi@sinap.ac.cn
Prof. X. C. Zeng
Department of Chemistry, University of Nebraska-Lincoln
Lincoln, NE 68588 (USA)

[**] This work was supported by the 973 program (2014CB845603), the Natural Science Foundation of China (21125102, 21390390, 21473139, and 21273268), China Postdoctoral Science Foundation (Y419022011).

Supporting information for this article is available on the WWW under http://dx.doi.org/10.1002/anie.201503893.

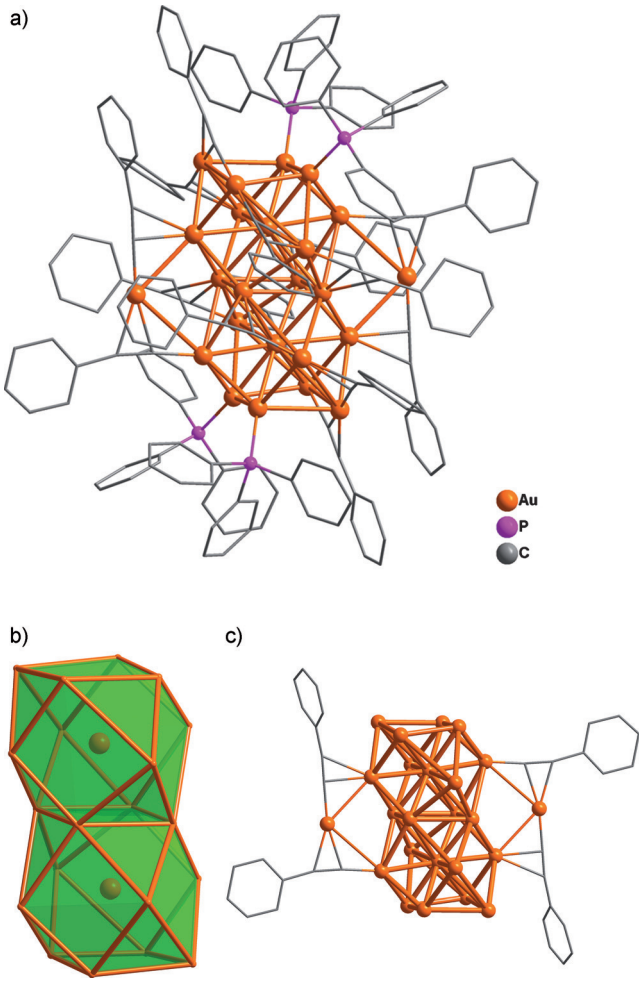

Figure 2. a) The molecular structure of **1**. b) The square-face-sharing Au_{22} double cuboctahedron. c) Two PhC≡C–Au–C≡CPh motifs attaching to the Au_{22} core.

in CD_2Cl_2 solution that shows only one singlet at $\delta = 40.2$ ppm (see Figure S1 in the Supporting Information). The other surface gold atoms are ligated by C≡CPh ligands.

As shown in Figure 2b, the Au_{22} core is structured in the form of a double cuboctahedra (that is, with two Au_{13} units sharing a square face). A centered cuboctahedron Au_{13} moiety is the basic unit of the face-centered cubic (fcc) lattice of bulk gold, which differs from the centered icosahedral Au_{13} unit frequently found in gold nanoclusters. This Au_{13} moiety is similar to that found in $[Au_{23}(SR)_{16}]$.[12a] The cuboctahdron in **1** is distorted, that is, the polyhedron is compressed over two opposite antiparallel triangles. Thus the Au···Au distances from the interstitial atom to its 12 surrounding gold atoms can be classified into two groups: shorter distances in the range of 2.7181(13)–2.7822(14) Å and longer distances in the range of 3.0595(14)–3.3898(14) Å. The shared-square Au_4 is actually a rectangle with two sides of length 2.7246(15) Å and the other two sides which each measure 2.9552(15) Å. Two gold atoms are linked to the double cuboctahedral core (Au···Au distance 3.4006 Å) via C≡CPh bridging ligands, forming two PhC≡C–Au–C≡CPh motifs.

The Au_{24} structure of **1** is completely different to the two previously reported Au_{24} nanoclusters. The structure of the mixed-ligand-protected cluster $[Au_{24}(PPh_3)_{10}(SC_2H_4Ph)_5X_2]^+$ (X = Cl, Br) is in the shape of biicosahedra with a missing center,[28] and the selenolate-protected cluster $[Au_{24}(SePh)_{20}]$ has a prolate Au_8 core wrapped with $Au_3(SeR)_4$ and $Au_5(SeR)_6$ moieties.[29] The distinct structural difference among these three Au_{24}-containing examples clearly indicates that the nature of the ligand affects the formation of individual nanoclusters. The formed nanoclusters are not only different in geometric structure but also vary in their number of valence electrons.

In the $Au(C{\equiv}CPh)_2$ motif in **1**, two C≡CPh ligands are in a perpendicular arrangement (Figure 3, motif A). This orientation is similar to the -RS–Au–SR- bridge found in gold–

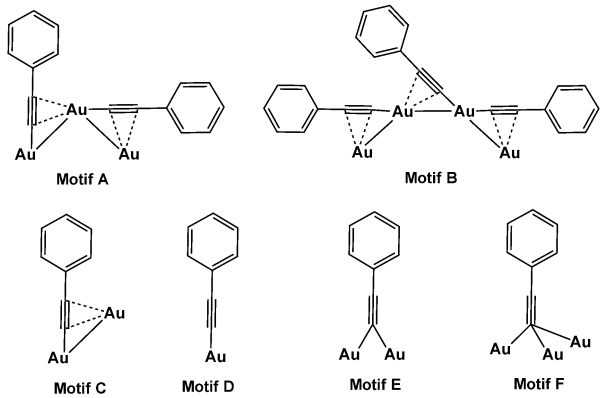

Figure 3. Reported bonding motifs for gold–alkynyl systems.

thiolate nanoclusters[6] and can be viewed as a mononuclear bridging unit in comparison with the dinuclear bridge (motif B) found in Au_{19} and Au_{23}.[24,25] The remaining ten C≡CPh ligands can be viewed as simple bridging groups (motif C), in which the C≡CPh ligand adopts a μ_2-bridging mode with a σ bond to one Au center and a π bond to another Au. The Au–C bond lengths for σ bonds are in the range of 1.93(3)–1.99(3) Å and those of π bonds are from 2.19(3) to 2.61(3) Å. These binding modes are different from those previously reported. Konishi et al. observed terminal monodentate bonding of the alkynyl to gold in the species $[Au_8(dppp)_4(C{\equiv}CR)_2]^{2+}$,[23] which is the σ binding (motif D). Extended X-Ray absorption spectroscopic analysis (EXAFS) by Tsukuda et al. suggested that the coordination modes of surface-bound alkynyl ligands are μ_2 (motif E) or μ_3 (motif F) modes.[22b]

The absorption spectrum of **1** in CH_2Cl_2 has a structured profile (Figure 4a). A weak shoulder appears at $\lambda = 425$ nm, which might arise from a transition involving contributions from both the metal and ligand. One prominent absorption band presents at $\lambda = 630$ nm, which is derived from metal-centered transitions. The optical energy gap is determined to be 1.75 eV (Figure 4a, inset). Figure 4b shows the computed absorption spectrum from time-dependent DFT (TDDFT) calculations. We can see that the extrapolated optical band

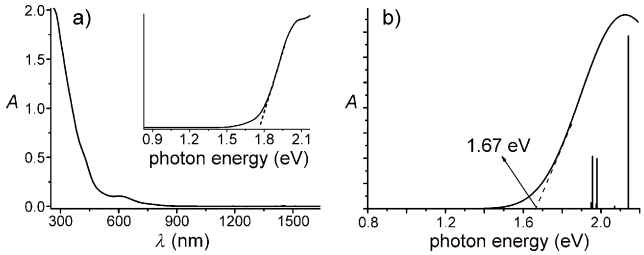

Figure 4. a) The experimental UV/Vis absorption spectrum of **1** and b) the computed spectrum of $[Au_{24}(C{\equiv}CCH_3)_{14}\{P(CH_3)_3\}_4]^{2+}$. The curve in (b) shows the TDDFT-computed spectrum obtained from the individual optical transitions (vertical lines).

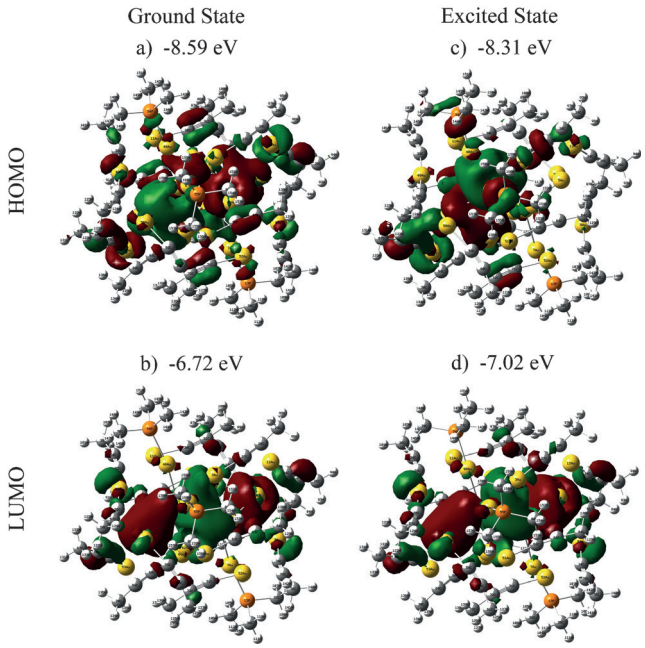

Figure 5. HOMO and LUMO distributions for a, b) the ground state and c, d) the first excited state of $[Au_{24}(C{\equiv}CCH_3)_{14}\{P(CH_3)_3\}_4]^{2+}$. The energies of the HOMO and LUMO (DFT/PBE computation) are also given. The isosurface value is set as 0.02.

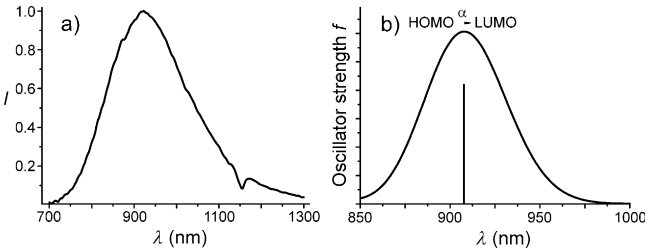

Figure 6. a) NIR photoluminescence spectrum of cluster **1** in CH_2Cl_2 ($\lambda_{exc} = 380$ nm). The solution was freshly prepared before measurement and a dilute solution (UV absorbance of about 0.1 at $\lambda = 600$ nm) was used to minimize self-absorbance and self-quenching effects. The intensity drop at 1150 nm is partly due to solvent/ligand absorption. b) The computed emission spectrum from TDDFT calculations. See the Supporting Information for computational details.

edge for $[Au_{24}(C{\equiv}CCH_3)_{14}(P(CH_3)_3)_4]^{2+}$ is 1.67 eV, very close to the measured value.

The number of valence electrons in cluster **1** is given by: $N^* = N_{Au} - N_{alkynyl} - N_{SbF_6^-} = 24 - 14 - 2 = 8$, a value which is in the magic number series for the superatom model. However, its shape is rod-like in contrast to the spherical shape predicted by superatom theory.[30] It is known that phosphine-protected rod-like Au_{20} nanoclusters have 14 valence electrons.[19] The charge distribution for the simpler species $[Au_{24}(C{\equiv}CCH_3)_{14}\{P(CH_3)_3\}_4]^{2+}$ has been computed (see Table S1 in the Supporting Information). These results suggest that the $P(CH_3)_3$ groups in the $Au{-}P(CH_3)_3$ moieties transfer electrons to Au atoms, contrary to the case of Au–S bonds in thiolate-covered Au clusters. Therefore the electronic structure of $[Au_{24}(C{\equiv}CCH_3)_{14}\{P(CH_3)_3\}_4]^{2+}$ cannot be normally viewed as a magic number cluster with eight free valence electrons. This is why the overall shape of $[Au_{24}(C{\equiv}CCH_3)_{14}\{P(CH_3)_3\}_4]^{2+}$ is not spherical but rod-like. Additionally, we also find that some electrons transfer from Au to the alkynyl groups (Table S1). From the HOMO of the ground state (in Figure S5), we find weak coupling between the s and d orbitals of the Au centers and the π* orbitals of the C≡C units, which induces a slightly longer bond length for C≡C within the species $[Au_{24}(C{\equiv}CCH_3)_{14}\{P(CH_3)_3\}_4]^{2+}$ (1.24 Å) compared with the conventional C≡C bond length of 1.20 Å.

The HOMO and LUMO plots shown in Figure 5 can offer additional insights into formation of the rod-like structure of $[Au_{24}(C{\equiv}CCH_3)_{14}\{P(CH_3)_3\}_4]^{2+}$, in which the large s-, p-, or d-type orbitals are not observed. The LUMOs of the ground state (Figure 5b) and the excited state (Figure 5d) are similar to one another, mainly because of the 6s orbitals of the Au_{14} unit (Figure S6). In contrast, the HOMO of the ground state (Figure 5a) and the excited state (Figure 5c) are composed mainly of orbitals of the Au_8 moiety (Figure S6a, red) and the Au_7 structure (Figure S6b, blue) of the gold core, respectively. These differences can be attributed to the more compact structure of the excited state than that of the ground state, which induces the Stoke's shift.

Cluster **1** emits strongly in the near-IR (NIR) region ($\lambda_{max} = 925$ nm) when excited with UV or visible radiation (Figure 6a), and the quantum yield was estimated to be 0.12 upon excitation at $\lambda = 380$ nm. It is noteworthy that strong-NIR-emissive gold nanoclusters are rare.[31,32] Figure 6b shows the calculated emission spectrum of $[Au_{24}(C{\equiv}CCH_3)_{14}\{P(CH_3)_3\}_4]^{2+}$ which was computed using the TDDFT method. The simulated NIR photoluminescence spectrum exhibits an emission maximum at $\lambda = 910$ nm, comparable to the experimental value at $\lambda = 925$ nm, and we attribute this band to originating from the HOMO–LUMO transition.

In summary, this work demonstrates that the combination of alkynyl and phosphine ligands is useful in the construction of new gold nanoclusters which show strong NIR emission in solution at room temperature. The detection of the new alkynyl binding motif PhC≡C–Au–C≡CPh provides valuable information for the design and structure prediction of similar metal-containing nanoclusters. We believe that by carefully tuning the synthetic parameters a variety of coinage-metal (including gold) nanoclusters can be generated by direct reduction of gold–alkynyl precursors.

Experimental Section

Synthesis of **1**: To a solution of Ph_3PAuCl (24.7 mg, 0.05 mmol) in $CHCl_3$ (4.0 mL), a solution of $AgSbF_6$ (17.2 mg) in methanol (0.1 mL) was added under vigorous stirring, leading to the immediate formation of a suspension. The reaction continued for 15 min at room temperature in the dark. The resulting solution was centrifuged for 4 min at 10000 rpm, and the AgCl precipitate was filtered off. After PhC≡CAu (44.7 mg, 0.15 mmol) was added to the filtrate, a freshly prepared solution of $NaBH_4$ (0.95 mg in 1.0 mL of ethanol) was added dropwise under vigorous stirring. The solution color changed from orange to pale brown and finally to dark brown. The reaction continued for 25 h at room temperature. A small amount of black solid appeared at the bottom of the flask. The mixture was evaporated to dryness to give a dark solid, which was dissolved in a mixed solvent CH_2Cl_2:CH_2Cl-CH_2Cl (V:V = 1:1) (1.6 mL). Excess ether was added to give a dark precipitate, which was collected by centrifugation. This crude solid was dissolved in a mixture of solvents CH_2Cl_2:ClH_2C-CH_2Cl (1:1 v/v; 1.6 mL), and the resulting solution was subjected to diffusion with ether to afford black crystals after two weeks.

Keywords: alkyne ligands · cluster compounds · DFT calculations · gold · photophysics

How to cite: *Angew. Chem. Int. Ed.* **2015**, *54*, 9683–9686
Angew. Chem. **2015**, *127*, 9819–9822

[1] G. Schmid, *Chem. Soc. Rev.* **2008**, *37*, 1909–1930.
[2] S. Yamazoe, K. Koyasu, T. Tsukuda, *Acc. Chem. Res.* **2013**, *46*, 816–824.
[3] G. Li, R. Jin, *Acc. Chem. Res.* **2013**, *46*, 1749–1758.
[4] M.-C. Daniel, D. Astruc, *Chem. Rev.* **2004**, *104*, 293–346.
[5] J. F. Parker, C. A. Fields-Zinna, R. W. Murray, *Acc. Chem. Res.* **2010**, *43*, 1289–1296.
[6] P. D. Jadzinsky, G. Calero, C. J. Ackerson, D. A. Bushnell, R. D. Kornberg, *Science* **2007**, *318*, 430–433.
[7] H. Qian, W. T. Eckenhoff, Y. Zhu, T. Pintauer, R. Jin, *J. Am. Chem. Soc.* **2010**, *132*, 8280–8281.
[8] D. Crasto, S. Malola, G. Brosofsky, A. Dass, H. Häkkinen, *J. Am. Chem. Soc.* **2014**, *136*, 5000–5005.
[9] C. Zeng, H. Qian, T. Li, G. Li, N. L. Rosi, B. Yoon, R. N. Barnett, R. L. Whetten, U. Landman, R. Jin, *Angew. Chem. Int. Ed.* **2012**, *51*, 13114–13118; *Angew. Chem.* **2012**, *124*, 13291–13295.
[10] a) C. Zeng, T. Li, A. Das, N. L. Rosi, R. Jin, *J. Am. Chem. Soc.* **2013**, *135*, 10011–10013; b) C. Zeng, C. Liu, Y. Chen, N. L. Rosi, R. Jin, *J. Am. Chem. Soc.* **2014**, *136*, 11922–11925.
[11] a) M. W. Heaven, A. Dass, P. S. White, K. M. Holt, R. W. Murray, *J. Am. Chem. Soc.* **2008**, *130*, 3754–3755; b) M. Zhu, C. M. Aikens, F. J. Hollander, G. C. Schatz, R. Jin, *J. Am. Chem. Soc.* **2008**, *130*, 5883–5885.
[12] a) A. Das, T. Li, K. Nobusada, C. Zeng, N. L. Rosi, R. Jin, *J. Am. Chem. Soc.* **2013**, *135*, 18264–18267; b) A. Das, C. Liu, H. Y. Byun, K. Nobusada, S. Zhao, N. Rosi, R. Jin, *Angew. Chem. Int. Ed.* **2015**, *54*, 3140–3144; *Angew. Chem.* **2015**, *127*, 3183–3187.
[13] a) Y. Pei, Y. Gao, X. C. Zeng, *J. Am. Chem. Soc.* **2008**, *130*, 7830–7832; b) Y. Pei, Y. Gao, N. Shao, X. C. Zeng, *J. Am. Chem. Soc.* **2009**, *131*, 13619–13621; c) Y. Pei, N. Shao, Y. Gao, X. C. Zeng, *ACS Nano* **2010**, *4*, 2009–2020; d) Y. Pei, R. Pal, C. Liu, Y. Gao, Z. Zhang, X. C. Zeng, *J. Am. Chem. Soc.* **2012**, *134*, 3015–3024; e) Y. Pei, X. C. Zeng, *Nanoscale* **2012**, *4*, 4054–4072; f) Y. Pei, J. Tang, X. Q. Tang, Y. Q. Huang, X. C. Zeng, *J. Phys. Chem. Lett.* **2015**, *6*, 1390–1395.
[14] a) Y. Gao, N. Shao, X. C. Zeng, *ACS Nano* **2008**, *2*, 1497–1503; b) W. W. Xu, Y. Gao, X. C. Zeng, *Sci. Adv.* **2015**, *1*, e1400211.
[15] S. Chen, S. Wang, J. Zhong, Y. Song, J. Zhang, H. Sheng, Y. Pei, M. Zhu, *Angew. Chem. Int. Ed.* **2015**, *54*, 3145–3149; *Angew. Chem.* **2015**, *127*, 3188–3192.
[16] a) C. Zeng, Y. Chen, K. Kirschbaum, K. Appavoo, M. Y. Sfeir, R. Jin, *Sci. Adv.* **2015**, DOI: 10.1126/sciadv.1500045; b) A. Dass, S. Theivendran, P. R. Nimmala, C. Kumara, V. R. Jupally, A. Fortunelli, L. Sementa, G. Barcaro, X. Zuo, B. C. Noll, *J. Am. Chem. Soc.* **2015**, *137*, 4610–4613.
[17] B. K. Teo, X. Shi, H. Zhang, *J. Am. Chem. Soc.* **1992**, *114*, 2743–2745.
[18] J. Chen, Q.-F. Zhang, T. A. Bonaccorso, P. G. Williard, L.-S. Wang, *J. Am. Chem. Soc.* **2013**, *135*, 92–95.
[19] X.-K. Wan, Z.-W. Lin, Q.-M. Wang, *J. Am. Chem. Soc.* **2012**, *134*, 14750–14752.
[20] X.-K. Wan, S.-F. Yuan, Z.-W. Lin, Q.-M. Wang, *Angew. Chem. Int. Ed.* **2014**, *53*, 2923–2926; *Angew. Chem.* **2014**, *126*, 2967–2970.
[21] B. S. Gutrath, I. M. Oppel, O. Presly, I. Beljakov, V. Meded, W. Wenzel, U. Simon, *Angew. Chem. Int. Ed.* **2013**, *52*, 3529–3532; *Angew. Chem.* **2013**, *125*, 3614–3617.
[22] a) P. Maity, H. Tsunoyama, M. Yamauchi, S. Xie, T. Tsukuda, *J. Am. Chem. Soc.* **2011**, *133*, 20123–20125; b) P. Maity, S. Takano, S. Yamazoe, T. Wakabayashi, T. Tsukuda, *J. Am. Chem. Soc.* **2013**, *135*, 9450–9457; c) P. Maity, T. Wakabayashi, N. Ichikuni, H. Tsunoyama, S. Xie, M. Yamauchi, T. Tsukuda, *Chem. Commun.* **2012**, *48*, 6085–6087.
[23] N. Kobayashi, Y. Kamei, Y. Shichibu, K. Konishi, *J. Am. Chem. Soc.* **2013**, *135*, 16078–16081.
[24] X.-K. Wan, Q. Tang, S.-F. Yuan, D.-e. Jiang, Q.-M. Wang, *J. Am. Chem. Soc.* **2015**, *137*, 652–655.
[25] X.-K. Wan, S.-F. Yuan, Q. Tang, D.-e. Jiang, Q.-M. Wang, *Angew. Chem. Int. Ed.* **2015**, *54*, 5977–5980; *Angew. Chem.* **2015**, *127*, 6075–6078.
[26] M. Brust, M. Walker, D. Bethell, D. J. Schiffrin, R. Whyman, *J. Chem. Soc., Chem. Commun.* **1994**, 801–802.
[27] Crystal data for **1**·4CH_2Cl_2: $C_{188}H_{138}Cl_8F_{12}P_4Sb_2Au_{24}$, a = 16.4792(10), b = 16.5176(11), c = 20.1042(10) Å, α = 73.904(5), β = 77.708(5), γ = 71.357(6)°, V = 4935.3(5) Å^3, triclinic, space group $P\bar{1}$, Z = 1, T = 173 K, 27341 reflections measured, 14473 unique (R_{int} = 0.0805), final R_1 = 0.1072, wR_2 = 0.2751 for 10702 observed reflections [$I > 2\sigma(I)$]. CCDC 1062124 (**1**) contains the supplementary crystallographic data for this paper. These data are provided free of charge by The Cambridge Crystallographic Data Centre.
[28] A. Das, T. Li, K. Nobusada, Q. Zeng, N. L. Rosi, R. Jin, *J. Am. Chem. Soc.* **2012**, *134*, 20286–20289.
[29] Y. Song, S. Wang, J. Zhang, X. Kang, S. Chen, P. Li, H. Sheng, M. Zhu, *J. Am. Chem. Soc.* **2014**, *136*, 2963–2965.
[30] M. Walter, J. Akola, O. Lopez-Acevedo, P. D. Jadzinsky, G. Calero, C. J. Ackerson, R. L. Whetten, H. Gronbeck, H. Häkkinen, *Proc. Natl. Acad. Sci. USA* **2008**, *105*, 9157–9162.
[31] Y. Shichibu, K. Konishi, *Small* **2010**, *6*, 1216–1220.
[32] G. Wang, T. Huang, R. W. Murray, L. Menard, R. G. Nuzzo, *J. Am. Chem. Soc.* **2004**, *126*, 812–813.

Received: April 28, 2015
Published online: June 26, 2015